

Cite this article as: Xu Kuixue, Liu Wei, Cheng Xi, et al. Friction Coefficient of a Novel Bionic Trabecular Bone[J]. Rare Metal Materials and Engineering, 2021, 50(08): 2777-2782.

ARTICLE

## Friction Coefficient of a Novel Bionic Trabecular Bone

Xu Kuixue<sup>1</sup>, Liu Wei<sup>1</sup>, Cheng Xi<sup>1</sup>, Pan Chao<sup>1</sup>, Wang Zhenguo<sup>1</sup>, Yuan Zhishan<sup>2</sup>, Wang Lvwu<sup>2</sup>

<sup>1</sup>Beijing Chunlizhengda Medical Instruments Co., Ltd, Beijing 101100, China; <sup>2</sup>GRIMED Medical (Beijing) Co., Ltd, Beijing 102200, China

**Abstract:** The coefficient of friction (COF) of a novel bionic trabecular structure that was manufactured through 3D printing with Ti-6Al-4V power was investigated. Cortical and spongy bones were used as counterparts. The contact angle results show that the bionic structure has better surface wettability than the homogeneous structure at the early-stage. However, the two structures have highly hydrophilic surface. For homogeneous trabeculae, the average values of COF range from 0.71 to 0.82, which are significantly lower than the values of 0.82~0.99 for the bionic trabeculae. The static COF values range from 1.52 to 1.96 for the bionic trabeculae and 0.99 to 1.26 for the homogeneous trabeculae. The maximum static COF value of 1.96 is acquired at 10 N for the cortical bone against the bionic trabeculae. The results indicate that the bionic trabecular structure has a higher COF than the homogeneous trabeculae and other components. Hence, the novel bionic trabecular structure can provide sufficient friction at the bone-implant interface, thus achieving primary stability.

**Key words:** biomaterials; COF; bionic trabecular bone; 3D printing

The primary stability of implants is an important factor for the successful implantation, and it is critical for osseointegration in primary and revision hip arthroplasty for acetabular components. It is affected by the architecture of the bone surrounding the implant, surgical technique, and implant geometry (length, diameter and surface characteristics)<sup>[1]</sup>. For implant manufacturers, there are ways to design and realize implant geometry. Additively manufactured porous metallic structures have recently received much attention in bone implant applications<sup>[2-4]</sup>. Electron beam melting (EBM) is one of the additive manufacturing technology for orthopedic implants, which is of interest for the fabrication of intricate geometries for cellular materials in areas where complex architectures are needed<sup>[5,6]</sup>.

Natural bones are porous materials with interconnected voids and consist of outer cortical bone and inner trabecular bone. Porous titanium materials with interconnected pores and porosities similar to those of natural bones are of particular interest for orthopedic implant applications<sup>[7]</sup>. And the pore interconnectivity is very important for the implants to show positive influence on osteoconductive properties of metallic implants<sup>[8]</sup>.

The mechanical properties of porous implants are close to those of host bone, which is expected to reduce the stress-shielding effect<sup>[9]</sup>. The porous structure is conducive to the adhesion, differentiation and growth of osteoblasts, promoting the growth of new bone into the pores, enhancing the combination of implant and bone, and achieving the fixation of implant and bone tissue. Moreover, the internal pores are conducive to vascularization and metabolic material transportation<sup>[10]</sup>. In addition, the porous structure has different coefficients of friction (COFs). The COF influences the mechanical stability of the implant, its relative motion, and the reaming and seating of the implant in the bone<sup>[11]</sup>. Harrison et al indicated that a higher COF is considered to be an advantage in providing improved primary fixation for orthopaedic implants<sup>[12]</sup>. For porous titanium acetabular components, to provide even greater interface friction for further improving initial mechanical stability, the surface roughness was increased<sup>[13]</sup>. Studies have also indicated that a highly porous acetabular cup with COFs between 0.8 and 1.2 is less influential given the plethora of other surgical implantation factors<sup>[14]</sup>.

Therefore, the key characteristics to design porous metallic

Received date: August 04, 2020

Foundation item: National Natural Science Foundation of China (51401027); China Postdoctoral Science Foundation (2016M591040)

Corresponding author: Wang Zhenguo, Ph. D., Senior Engineer, Beijing Chunlizhengda Medical Instruments Co., Ltd, Beijing 101100, P. R. China, E-mail: wzghappy@yeah.net

Copyright © 2021, Northwest Institute for Nonferrous Metal Research. Published by Science Press. All rights reserved.

implants include the selection of porosity, pore size, and pore interconnectivity, aiming to achieve satisfactory clinical outcomes<sup>[15]</sup>. As a novel concept for bone implant prostheses, porous trabecular bone implants have become a focus of research and clinical attention, especially the bio-inspired design.

However, fabrication of porous titanium implants with mechanical properties suitable to mimic natural bones, especially the bionic trabecular structure, is still a challenge. Hence, in this study, a novel bionic trabecular structure was designed by CAD molding to natural bones, which was 3D-printed with Ti-6Al-4V powder by EBM. The COFs between the bionic trabecular structure and bone were investigated.

## 1 Experiment

Small specimens (10 mm×10 mm×10 mm) used as substrates were cut from 2D-C/C composites with a density of 1.78 g/cm<sup>3</sup>. The specimens were hand-polished using 400 grit sand paper, then cleaned with alcohol and dried in air. Powder compositions in mass fraction for pack cementation process were as follows: 75%~80% Si (45 μm) and 20%~25% graphite (45 μm) for SiC coating, 60%~75% Si (45 μm), 20%~30% Ta (45 μm) and 5%~10% graphite (45 μm) for TaSi<sub>2</sub> coating. The pack mixtures were weighed and mixed by tumbling in a ball mill up to 10 h. For comparison, homogeneous and bionic trabecular structures were designed by research engineers. The three-dimensional structures of both the homogeneous and bionic trabecular structure were first drawn using 3D-CAD software 3-matic. When using the 3D-CAD design, the default parameters were entered, and the 3D-CAD design drawings are shown in Fig. 1a and 1c. Fig. 1a is the homogeneous structure and Fig. 1c is the bionic structure. The drawings were fabricated by Ti-6Al-4V powder using an Arcam Q10 plus EBM machine. The particle size of Ti-6Al-4V powder distribution is between 45 and 106 μm. Fig. 1b and 1d show the 3D-printed samples produced via EBM. Table 1 presents the porosity, pore size and trabecular thickness for the homogeneous and bionic trabecular structures.

Initial contact angle analysis was performed to characterize

**Table 1 Porosity, pore size and trabecular thickness**

Structure	Porosity/%	Pore size/μm	Trabecular thickness/mm
Homogeneous	~62.5	~300	~2
Bionic	50~80	200~400	300~700

the variation of surface wettability through an optical contact angle measuring instrument (DSA 100S, Germany). Digital images were taken perpendicular to the 5 μL droplets of ultrapure water placed on the surface, and the angle tangential to the water-surface interface was directly measured from each image.

The friction tests were carried out on a commercial reciprocating tribotester (Cetr UMT-2). All the experimental tests were performed at an ambient temperature of approximately 25 °C. The reciprocating stroke was 15 mm, which corresponds to a sliding frequency of 1/60 Hz. Normal loads of 5, 10 and 15 N were used. The counterparts employed during the test were 6 mm in diameter and 15 mm in height and made of cortical bone and spongy bone. The cortical and spongy bones were obtained through a milling machine from pork bones, and the contact surface was polished by 3000# SiC abrasive paper. The surface roughness was 0.82±0.11 and 0.91±0.15 μm for the cortical bone and spongy bone, respectively. To prevent bone breakage during testing, the clamped position for the bone was packed by waterproof adhesive tape. The lubricating fluid in this procedure was newborn calf serum at a concentration of 20 g/L. In order to ensure the consistency of the tests, the samples were completely immersed in the lubricating fluid in the testing process. During the tests, the COFs were recorded by the computer. Experiments were performed in triplicate for each test under different conditions.

## 2 Results and Discussion

The surface wettability of biomaterials is one of the most decisive aspects governing the cell adhesive properties. Droplet images taken during the measurements are shown in

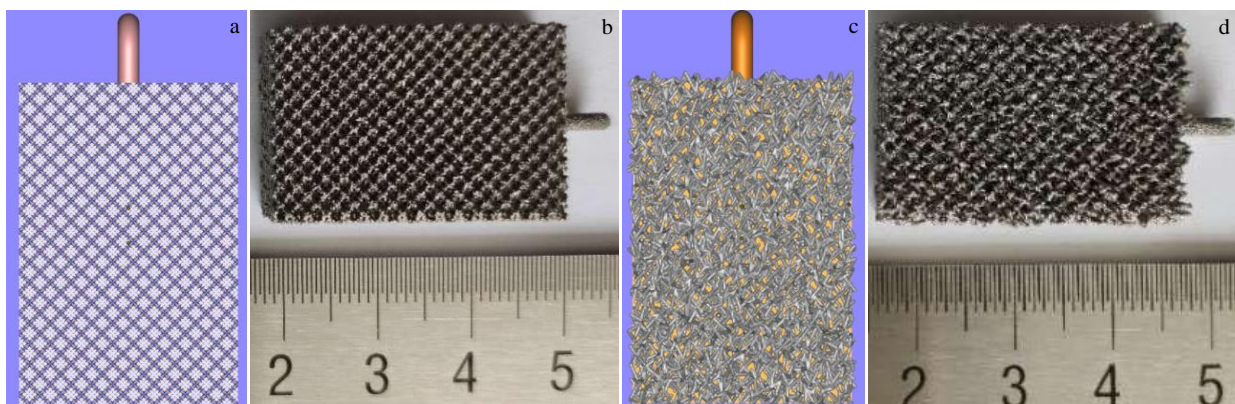


Fig.1 Homogeneous (a, b) and bionic (c, d) trabecular bone structures: (a, c) 3D-CAD design and (b, d) 3D-printed

Fig.2. Fig.2a shows that the initial contact angle is about  $96.9^\circ$  for the homogeneous structure, while the bionic structure has a lower initial contact angle of  $87.7^\circ$ , as shown in Fig.2b. The result shows that the bionic structure has better surface wettability than the homogeneous structure at the early-stage. The contact angles are reported to be zero due to inherent surface roughness for the two different structures. That is, the two structures has highly hydrophilic surface, and it will increase the early-stage bone tissue integration or osseointegration<sup>[16]</sup>. It has been reported that implants exhibiting a higher degree of surface wettability can promote adhesion of proteins, interstitial fluid, and blood macromolecules, which can further improve biological integration and result in faster healing for patients<sup>[17,18]</sup>.

Fig.3 presents the COFs of the homogeneous/bionic trabeculae under different experimental conditions. The average COFs are listed in Table 2. The average COF increases with increasing the load. This may be due to the increase in area of contact between the sample and bone surface. Due to the increased area of contact, there is more interaction between bone trabeculae or asperities, which results in increased COF<sup>[11]</sup>. For the homogeneous trabeculae, the values ranging from 0.71 to 0.82 are obviously lower than the values of 0.82~0.99 for bionic trabeculae. The max average COF of 0.99 is obtained for the cortical bone against the bionic trabeculae at 15 N. Some studies have shown that high COF between implant and bone enhances the initial stability with small micro motions at the interface<sup>[9,11,13]</sup>. The trabecular structure has a larger attachment surface of bone cells and greater surface energy, which is conducive to adsorption of macromolecules on cells and bone tissue, leading to bony on-

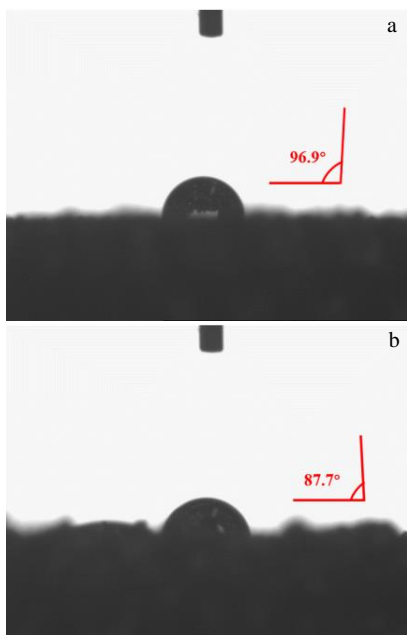


Fig.2 Initial surface contact angle of homogeneous (a) and bionic (b) structures

growth<sup>[12]</sup>.

The static COF between the sample and bone is needed, and it is more representative for the tribological properties of the trabeculae structure. As shown in Fig. 3, the first COF peak value is defined as the static COF<sup>[19]</sup>; the values are also listed in Table 2. The first COF peak value increases with increasing the load. The values range from 1.52 to 1.96 for the bionic trabeculae, larger than the values from 0.99 to 1.26 for the homogeneous trabeculae. When the friction pair is the cortical bone and bionic trabeculae, the maximum static COF value of 1.96 is acquired at 10 N. The first COF peak values are significantly larger than those of trabecular structures that were designed by other companies, such as the values of 0.8~1.2 for DePuy products<sup>[20]</sup> and 0.93~1.08 for the 3D ACT trabecular structure. The higher COF is attributed to the uneven trabecular structure at the interface hindering the motion of the mating surface along the surface<sup>[21]</sup>. The results indicate that the bionic trabeculae can enhance the initial stability of implants, effectively prevent the prosthesis from fretting and sinking and promote long-term stability. Previous research has shown that a higher COF enhances interference fit and ultra-porous surfaces enhance osseointegration<sup>[22]</sup>. Another study showed that high friction and porosity can minimize micro motion and diminish possible fibrous texture formation around the revision implant<sup>[23]</sup>.

However, it is reported that a higher COF does not necessarily translate to greater stability, and the COF affects the final position of the implant under a given implantation force<sup>[24]</sup>. A study pointed out that the COF of the acetabula cup plays a limited role compared with the factor of bone quality in resisting relative micro motion in the cup-pelvis interface<sup>[25]</sup>.

It is evident in Fig.3 that there are large fluctuations in all the curves. The curves are related to the implant surfaces with different structures. One study found that by introducing gradient variation in surface microstructures, more novel materials with tunable frictional properties can be designed and fabricated<sup>[26]</sup>, and the trabecular structures used in this study are based on this consideration. The variation in the curves in Fig.3 reflects the changes in the trabecular structure. Although the fluctuation in the curves is large, the friction remains at a high level. Sufficient frictional stability enables bone in-growth into the surface of the implant, resulting in a long-lasting mechanical interlock of the implant and optimal secondary mechanical stability<sup>[13]</sup>.

Fig. 4 shows the bone debris on the homogeneous/bionic trabecular surface after the tests. There is significantly more spongy bone debris than cortical bone debris. This is dependent on the structure and density of the bone. In addition, the amount of bone debris on the bionic trabecular surface is larger than on the homogeneous trabecular surface. This is mainly due to different trabecular structures. The results indicate that the bionic trabeculae results in more friction than the homogeneous trabeculae. In other words, the bionic trabecular has a higher COF than homogeneous trabeculae.

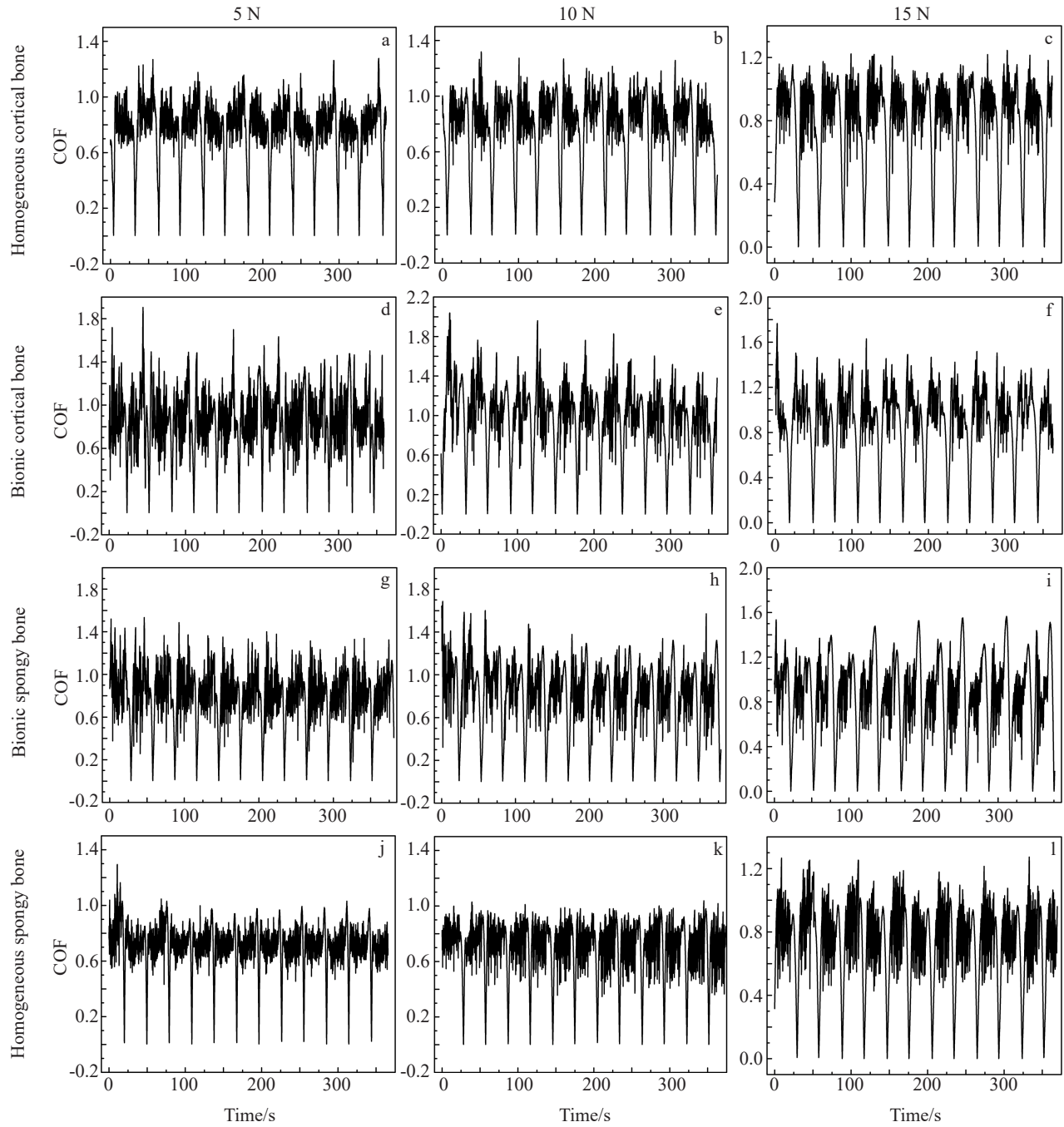


Fig.3 COFs of homogeneous and bionic trabeculae under loads of 5 N, 10 N, and 15 N: (a~f) cortical bones and (g~l) spongy bones

Table 2 Average and static COFs

Bone	Structure		5 N	10 N	15 N
Spongy	Homogeneous	Average	0.71	0.72	0.76
		Static	1.04	0.99	1.26
	Bionic	Average	0.82	0.85	0.88
		Static	1.52	1.68	1.53
Cortical	Homogeneous	Average	0.77	0.79	0.82
		Static	1.07	1.03	1.16
	Bionic	Average	0.88	0.99	0.91
		Static	1.71	1.96	1.76

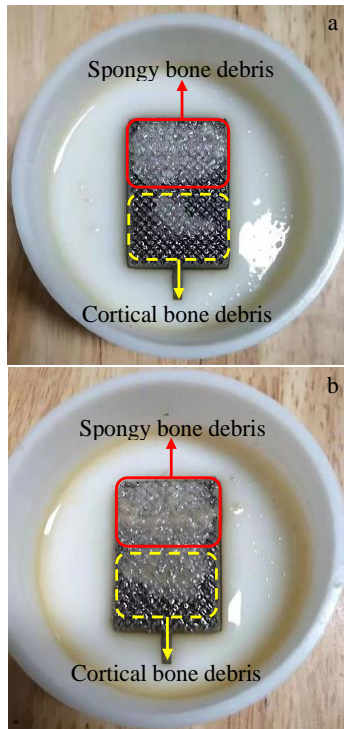


Fig.4 Bone debris on the trabecular surface: (a) homogeneous and (b) bionic

### 3 Conclusions

1) The COFs of the bionic and homogeneous trabecular structures are investigated in a newborn calf serum fluid. The initial contact angle is about  $96.9^\circ$  for the homogeneous structure, which is higher than that of the bionic structure ( $87.7^\circ$ ). The bionic structure has better surface wettability than the homogeneous structure at the early-stage.

2) The COF increases as the load increases. For the bionic trabeculae, the average COFs range from 0.82 to 0.99, which are higher than the values of 0.71~0.82 for the homogeneous trabecular. Similarly, the static COF values are 1.52~1.96 for the bionic trabeculae, which are significantly higher than the values of 0.99~1.26 for the homogeneous trabeculae. The maximum static COF of 1.96 is acquired at 10 N in the test between the cortical bone and bionic trabecular. The bionic trabecular structure has a higher COF.

3) The newly developed bionic trabecular structure can provide sufficient friction at the bone-implant interface, thus achieving primary stability due to a higher friction coefficient.

### References

- 1 Ovesy M, Indermaur M, Zysset P K. *Journal of the Mechanical Behavior of Biomedical Materials*[J], 2019, 98: 301
- 2 Thomas D, Singh D. *International Journal of Surgery*[J], 2017,

- 46: 195
- 3 Weißmann V, Bader R, Hansmann H et al. *Materials and Design* [J], 2016, 95: 188
- 4 Bartolomeua F, Douradoa N, Pereira F et al. *Materials Science & Engineering C*[J], 2020, 107: 110 342
- 5 Ibrahim E, Ola Harrysson Harvey We et al. *Additive Manufacturing*[J], 2017, 17: 169
- 6 Hernández-Navaa E, Smitha C J, Derguti F et al. *Acta Materialia* [J], 2016, 108: 279
- 7 Yan C Z, Hao L, Hussein A et al. *Journal of the Mechanical Behavior of Biomedical Materials*[J], 2015, 51: 61
- 8 Bandyopadhyay A, Espana F, Balla V K et al. *Acta Biomaterialia* [J], 2010, 6(4): 1640
- 9 Hu Y B, Li J Z. *Journal of Materials Processing Technology*[J], 2017, 249: 426
- 10 Kang C W, Fang F Z. *Advances in Manufacturing*[J], 2018, 6: 137
- 11 Aziz R, Haq M I U, Raina A. *Polymer Testing*[J], 2020, 85: 106 434
- 12 Harrison N, McHugh P E, Curtin W et al. *Journal of the Mechanical Behavior of Biomedical Materials*[J], 2013, 21: 37
- 13 Small S R, Berend M E, Howard L A et al. *Journal of Arthroplasty*[J], 2013, 28(3): 510
- 14 Goldman A H, Armstrong L C, Owen J R et al. *Journal of Arthroplasty*[J], 2016, 31(3): 721
- 15 Wang Xiaojian, Xue Shanqing, Zhou Shiwei et al. *Biomaterials* [J], 2016, 83: 127
- 16 Sartoretto S C, Alves A T, Resende R F et al. *Journal of Applied Oral Science*[J], 2015, 23(3): 279
- 17 Rupp F, Gittens R A, Scheideler L et al. *Acta Biomaterialia*[J], 2014,10(7): 2894
- 18 Sabetrsek R, Tiainen H, Reseland J E et al. *Biomedical Materials*[J], 2010, 5(1): 15 003
- 19 Luo Y, Yang L, Tian M C. *Biomaterials and Medical Tribology* [J], 2013: 181
- 20 Biemond J E, Aquarius R, Verdonschot N et al. *Archives of Orthopaedic and Trauma Surgery*[J], 2011, 131(5): 711
- 21 Majumdar D D, Ghosh M, Mondal D P et al. *Procedia Manufacturing*[J], 2019, 35: 833
- 22 Carli A V, Warth L C, Bentley K L M et al. *Journal of Arthroplasty* [J], 2017, 32(2): 463
- 23 Zhang C Q, Zhang L, Liu L et al. *Journal of Orthopaedic Surgery and Research* [J], 2020, 15: 40
- 24 Damm N B, Morlock M M, Bishop N E. *Journal of Biomechanics*[J], 2015, 48(12): 3517
- 25 Hsu J T, Chang C H, Huang H L et al. *Medical Engineering and Physics*[J], 2007, 29(10): 1089
- 26 Yuan W F, Yao Y, Keer L et al. *Extreme Mechanics Letters*[J], 2019, 26: 46

## 一种新型仿生骨小梁的摩擦系数

许奎雪<sup>1</sup>, 刘 伟<sup>1</sup>, 程 曦<sup>1</sup>, 潘 超<sup>1</sup>, 王振国<sup>1</sup>, 袁志山<sup>2</sup>, 王吕武<sup>2</sup>

(1. 北京市春立正达医疗器械股份有限公司, 北京 101100)

(2. 有研医疗器械(北京)有限公司, 北京 102200)

**摘 要:** 研究了一种新型仿生骨小梁结构的植入物的摩擦系数, 该新型骨小梁结构采用Ti-6Al-4V合金粉末进行3D打印制备。从牛骨中取皮质骨和松质骨作为摩擦配副。从2种结构的起始接触角测试结果可知, 仿生结构的接触角(87.7°)要比均匀骨小梁结构的接触角(96.9°)小一些, 说明其表面润湿性相对较好。对于均匀骨小梁结构而言, 其平均摩擦系数在0.71~0.82之间, 明显低于仿生骨小梁结构的摩擦系数(0.82~0.99)。均匀骨小梁结构的最大静摩擦系数为0.99~1.26, 而仿生骨小梁结构的最大静摩擦系数为1.52~1.96。仿生骨小梁的最大静摩擦系数1.96是在加载为10 N, 摩擦配副为皮质骨时获得的。结果表明, 新型仿生骨小梁结构的摩擦系数明显高于均匀骨小梁结构。因此, 新型仿生骨小梁结构可以在骨-种植体界面提供足够的摩擦力, 从而实现植入物初步稳定性。

**关键词:** 生物材料; 摩擦系数; 仿生骨小梁; 3D打印

---

作者简介: 许奎雪, 男, 1986年生, 硕士, 高级工程师, 北京市春立正达医疗器械股份有限公司, 北京 101100, E-mail: xukuixue@clzd.com